Biosensors and Bioelectronics 83 (2016) 339–346

Contents lists available at ScienceDirect

Biosensors and Bioelectronics

journal homepage: www.elsevier.com/locate/bios

Graphene modified screen printed immunosensor for highly sensitive detection of parathion

Jyotsana Mehta [a,b], Priya Vinayak [a,c], Satish K. Tuteja [a], Varun A. Chhabra [d], Neha Bhardwaj [a,b], A.K. Paul [a], Ki-Hyun Kim [e,*], Akash Deep [a,b]

[a] Central Scientific Instruments Organisation (CSIR-CSIO), Sector 30 C, Chandigarh 160030, India
[b] Academy of Scientific and Innovative Research, CSIR-CSIO, Sector 30 C, Chandigarh 160030, India
[c] UIET, Panjab University, Sector 14, Chandigarh 160014, India
[d] Centre for Development of Advanced Computing, Phase VIII, Mohali 160071, India
[e] Department of Civil & Environmental Engineering, Hanyang University, 222 Wangsimni-Ro, Seoul 04763, Republic of Korea

ARTICLE INFO

Article history:
Received 18 February 2016
Received in revised form
18 April 2016
Accepted 19 April 2016
Available online 20 April 2016

Keywords:
Graphene
Impedance
Parathion
Sensing
Screen-printed electrode

ABSTRACT

Due to indiscriminate use of pesticides, there is a growing need to develop sensors that can sensitively detect the trace amount of pesticides in food and water samples. Parathion, identified as an acetylcholinesterase inhibitor, had been one of the most widely used pesticides throughout the world. Symptoms of its poisoning are found to be diverse enough to include nausea, vomiting, diarrhea, muscle cramping/twitching, and shortness of breath. In this work, a graphene based impedimetric immunosensor has been fabricated and employed for highly sensitive and specific detection of parathion. The fabrication proceeded through the modification of the screen-printed carbon electrodes (SPE) with graphene sheets, followed by their functionalization with 2-aminobenzyl amine (2-ABA) via an electrochemical reaction. These amine functionalized graphene electrodes were then bio-interfaced with the anti-parathion antibodies. In the impedimetric mode, this biosensor detected parathion in a broad linear range, i.e. 0.1–1000 ng/L with a very low limit of detection (52 pg/L). It also showed high selectivity towards parathion in the presence of malathion, paraoxon, and fenitrothion. The viability of this biosensor was demonstrated by detecting parathion in real samples (e.g., tomato and carrot) and through cross-calibration against HPLC.

1. Introduction

Different classes of pesticides, including organophosphates, organochlorides, carbamates, pyrethrums, and triazines are used extensively to combat agricultural pests (Aragay et al., 2012). Due to unsystematic use of these pesticides, their residues accumulate in the food chain and ultimately find their way to human consumers though water, food, and soil (Audrey et al., 2012). The organophosphates (OPs) are one of the most widely used classes of pesticides (approximately 36%) (Sukirtha and Usharani, 2013). Their toxicity effects in vertebrates are well documented (Aslan et al., 2011). The OPs are known to inhibit the activity of the essential acetylcholinesterase (AChE) enzyme, consequently posing various health risks, e.g. nerve disorders, respiratory diseases, and sometimes even death (Liu and Lin, 2005; Singh et al., 1999). Parathion is still recorded as one of the most commonly used OPs in developing counties like India (Consumer Resources, India, 2015). Therefore, a routine and a convenient detection of parathion is essential to maintain the quality of the food and water human consumes.

High performance liquid chromatography (HPLC) and gas chromatography–mass spectroscopy (GC–MS) are the common techniques for the qualitative and quantitative detection of pesticides (Du et al., 2010; Wen et al., 2010). The above methods are time consuming and costly while producing large amounts of organic waste. Hence, they are not necessarily preferable options for an on-field real time monitoring (Liu and Lin, 2005). During the last two decades, the biosensors have gained considerable analytical interest for the determination of pesticides due to advantages of portability, routine detection, and fast processing time (Mulchandani et al., 2001). Different biosensing platforms are categorized on the basis of the type of the bio-recognizing element (e.g., antibody, protein, enzyme, and microorganism) and or the transduction unit (e.g. optical, piezoelectric, and electrochemical)

* Corresponding author.
E-mail addresses: kkim61@hanyang.ac.kr (K.-H. Kim), dr.akashdeep@csio.res.in (A. Deep).

http://dx.doi.org/10.1016/j.bios.2016.04.058
0956-5663/

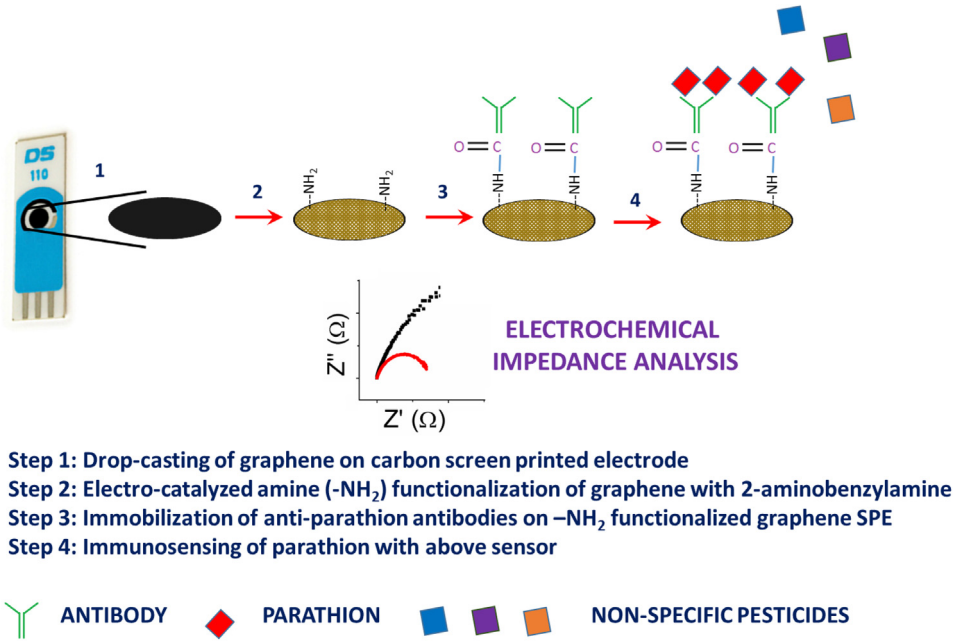

Fig. 1. Schematic of the graphene-based, screen-printed immunosensor for parathion.

(Bontidean et al., 2003; Cherian et al., 2003; Dzyadevych et al., 2003; Khosraviani et al., 1998; Mattiasson, 1997; Preininger and Wolfbeis, 1996). Electrochemical signaling based biosensors are immensely popular due to their sensitivity, selectivity, rapid response, and low-cost manufacturing (Takahashi et al., 2010; Goicolea et al., 2011). Various electrochemical biosensors have been proposed for the detection of OPs based on amperometry, potentiometry, voltammetry, and impedance analysis (Wu et al., 2013; Xue et al., 2013; Bhardwaj et al., 2015; Deep et al., 2015; Zhao et al., 2015; Chauhan et al., 2016). The electrochemical impedance spectroscopy (EIS) is an interesting class of the electrochemical techniques with an underlying capability of direct analyte detections via simple affinity complex formation. The EIS measurements involve the study of charge transfer resistance or capacitance at the electrode interface during probe-analyte interaction (Bourigua et al., 2010). The extension of EIS-based sensors to screen-printed electrodes is used to realize compact and cost-effective detection systems (Arora et al., 2011).

Recent developments in nanomaterials have made it possible to further improve the sensitivity levels of the pesticide biosensors (Rosi and Mirkin, 2005; Du et al., 2009; Aragay et al., 2012; Audrey et al., 2012; Kumar et al., 2012, 2015; Li et al., 2012; Bhardwaj et al., 2015; Deep et al., 2015). Several studies have established graphene as a material of choice for the construction of highly sensitive and stable biosensors for a variety of analytes (Suri et al., 2009; Shao et al., 2010; Yola et al., 2014a, 2014b, 2016; Tuteja et al., 2015; Atar et al., 2016). Graphene is characterized with ultra-high charge mobility, high surface to volume ratio, high Young's modulus, and excellent target binding properties, which together result in enhanced selectivity and sensitivity (Wang et al., 2010, 2013; Atar et al., 2015). Various types of graphene containing nanoconjugates have also been widely explored for the sensing of different analytes (Akyıldırım et al., 2015; Yola et al., 2015; Kotan et al., 2016;).

The use of graphene for the development of pesticide biosensors has been reported for organophosphates and carbamates (Gong et al., 2011, 2012; Liu et al., 2011a, 2011b; Wu et al., 2013). Most of these sensors exploited the use of graphene in a nanocomposite form with other materials (Gong et al., 2011, 2012; Liu et al., 2011a, 2011b; Wu et al., 2013) and the related measurements relied on the mechanism of inhibition of the bio-immobilized enzyme's activity. In some studies, the graphene nanostructures have also been used to design screen printed biosensors (SPE) (Ping et al., 2011; Song et al., 2013; Yang et al., 2013). Ping et al. (2011) proposed the assembly of a reduced graphene oxide/ionic-liquid doped SPE for the biosensing of glucose with the aid of physically immobilized glucose oxidase. As another example, a chitosan-reduced graphene oxide–nickel nanocomposite was deposited on an SPE to realize an enzyme-free detection of glucose (Yang et al., 2013). A silver nanoparticles/graphene modified SPE has also been proposed for the sensing of immunoglobulin E (Song et al., 2013). The SPE had to be conjugated with a specific aptamer (bio-recognition molecule) via streptavidin beads. Recently, a graphene modified SPE has also been proposed for the analysis of cathecholamine neurotransmitter (Apetrei et al., 2014). These authors attached the required enzymatic bioprobe on the graphene surface via glutaraldehyde mediated conjugation process.

In this research, we explored the viability of a convenient graphene-SPE platform for non-enzymatic label-free immunosensing of parathion. Unlike the approaches employed in earlier reports, the herein used graphene SPE does not need any mixing with other materials. The bioconjugation process has also been straightforwardly performed without the use of cross linkers or any other cumbersome chemistry. Briefly, the SPE was first modified with the dispersed graphene sheets. The electrode surface was then electrochemically treated with the 2-aminobenzyl amine so as to generate the active $–NH_2$ functional groups. The above functionalized electrodes were then simply incubated with the anti-parathion antibodies to realize the desired biosensor. As the antibody molecules were bound to the graphene-modified SPE through the F_c region based on this approach, this oriented immobilization allowed the biosensor to have free F_{ab} regions of the bio-recognizing probe. As such, enhanced detection sensitivity of this biosensor is expected to be achieved by activating all the possible available antibody probes in the system. A full scheme of this proposed strategy is illustrated in Fig. 1. The developed graphene SPE immunosensors has offered a highly sensitive and a specific electrochemical detection of parathion.

2. Experimental section

2.1. Reagents and chemicals

All chemicals used in the study were of analytical reagent grade purity. Single-layer graphene sheets were purchased from ACS Chemicals (USA); 2-aminobenzyl amine '2-ABA' and parathion were purchased from Sigma Aldrich (India). Anti-parathion antibodies (Rabbit polyclonal) and screen-printed carbon electrodes (Dropsens make) were purchased from Abcam (India) and Metrohm (India), respectively.

2.2. Material characterizations

Spectroscopic characterizations of graphene and its bioconjugate were studied by Fourier transform infrared (FTIR) spectroscopy (Nicolet iS10, USA) and UV–vis spectroscopy (Varian Cary 5000). Field-emission scanning electron microscopy (FE-SEM) investigations and electrochemical measurements were carried out using Hitachi S4300/SE system (Hitachi, Japan) and PGSTAT302N system (Autolab, Netherlands), respectively. The surface topography of the electrodes was studied by atomic force microscopy (AFM, XE-NSOM, Park Systems). Fluorescence imaging was carried out on a confocal laser scanning microscope (CLSM, LSM, Zeiss).

2.3. Functionalization of graphene with 2-ABA

Single-layer graphene sheets were first carboxylated by ultrasonication of a 50 mg sample in 30 mL of H_2SO_4/HNO_3 (3/1, v/v) for 4 h (Chhabra et al., 2012). The product was filtered through hydrophilic (0.22 μm) filter paper after appropriate dilution and then washed with distilled water. The sample was vacuum dried at 50 °C.

For the modification of SPE with graphene, ethanolic slurry of carboxylated sample was drop-casted over the working electrode area. The remaining counter and reference electrodes were properly masked with removable tape. The graphene-cast SPE electrodes (G-SPE) were annealed at 100 °C for 60 min to improve the cohesiveness of the graphene sheets. As reported earlier, the annealing process should not interfere with functionality of the processed graphene sheets (Jeon et al., 2012). Further functionalization of the G-SPE with 2-ABA was performed via an electrochemical process using an electrolyte solution of 10 mM 2-ABA (in PBS buffer, pH=7.4). A fixed potential of 0.5 V was applied for 5 min The electrolytic deposition of 2-ABA on graphene surface took place through interatomic binding between the carboxyl groups of graphene sheets and amine groups of 2-ABA (Tuteja et al., 2015). After functionalization (with $–NH_2$), the resulting electrodes (fG-SPE) were washed with water and then vacuum dried.

2.4. Conjugation of anti-parathion antibody (Ab) on $–NH_2$ functionalized graphene screen-printed electrode (fG-SPE)

For bio-interfacing of fG-SPE electrodes with the anti-parathion antibody, a 100 μL of antibody solution (0.1 mg/mL) was first incubated with 100 μL of freshly prepared EDC + sulfo-NHS (0.1 mM) for 30 min at room temperature. This mixture was then drop-cast over the working electrode areas of the G-SPE, followed by incubation at 4 °C for 1 h. The immobilization of the anti-parathion antibodies on the fG-SPE occurred through amide bond formation. The resulting antibody-conjugated electrodes (Ab-fG-SPE) were rinsed with Tween 20-PBS mixture (0.01% Tween 20, pH 7.4) to remove the unbound antibody molecules. These electrodes were subsequently incubated with BSA (0.1 mg/mL in PBS buffer) solution for 30 min in order to block non-specific antibody sites. The above obtained multiple Ab-fG-SPE electrodes were stored at 4 °C. Note that the F_c chains of the antibody molecules were used during the above immobilization step. Hence, the oriented availability of F_{ab} binding sites should facilitate high sensitivity of the immunosensor.

2.5. Electrochemical studies

The electrochemical impedance spectroscopic (EIS) measurements were performed using an electrolyte of 10 mM potassium ferricyanide and potassium ferrocyanide in PBS, i.e., 10 mM $[Fe(CN)_6]^{3-/4-}$ as the redox couple. The impedance data were recorded during different steps of functionalization, immobilization, and analyte detection. Nyquist plots were recorded in a frequency range of 1 KHz–1 MHz at a fixed potential of 0.5 mV. The detection of parathion was investigated in a dynamic concentration range of 0.01–10^4 ng/L. A 10 μL aliquot of each of these solutions was exposed to the Ab-fG-SPE electrodes. After 10 min, the sensor was washed with PBS and the electrochemical measurements were recorded. Cyclic voltammetry studies were also performed using 10 mM $[Fe(CN)_6]^{3-/4-}$ electrolyte as the redox couple maintaining a scan rate of 0.1 V/s.

3. Results and discussion

3.1. Spectroscopic and structural characterizations

The successful carboxylation of graphene and the subsequent immobilization of the antibodies was confirmed using FTIR and UV–vis spectroscopic studies. FTIR spectra of the pristine and carboxylated graphene are shown in Fig. 2. The peaks around 1578 and 3300 cm^{-1} (weak stretching) can be ascribed to the skeletal vibrations and adsorbed water molecules, respectively. A small band around 1660 cm^{-1} was due to the aromatic C=C bonds, while that at 1412 cm^{-1} can be assigned to the C–O bonds. The successful carboxylation was evident by the presence of bands around 1760–1620 (carbonyl stretch C=O) and 1050 cm^{-1} (O=C-OH). The FTIR signal around 1450 cm^{-1} can be attributed to the O-H bending. FTIR studies of the above electrode (G-SPE) after the electrochemical functionalization with 2-ABA is also shown in Fig. 2. These measurements were conducted in the attenuated total reflectance mode. A band around 1573 cm^{-1} along with some other signals around 1000–1250 cm^{-1} highlighted the N–H bending and C–N bond stretching as a result of the $–NH_2$ functionalization. Some other peaks around 3200–3400 cm^{-1} also suggested the N–H stretching for the $-NH_2$ modified graphene.

The bio-interfacing of graphene with the anti-parathion antibodies was also confirmed from the FTIR results. The amide absorption and C-N bond stretching, as characteristics of the amide bond formation between the $-NH_2$ functionalized graphene and the antibodies, were highlighted by the weakening of bands at 1615 and 1050–1300 cm^{-1}, respectively. A broad band near 3200 cm^{-1} representing N-H stretching (amide formation) further suggested the modification of graphene with antibody molecules.

UV–vis studies were carried out to assess the effect of carboxylation and antibody functionalization on the graphene sheets (Fig. 2 inset). Dispersed graphene showed a peak at 230 nm due to π- π* plasmons for nanoscale sp^2 C=C aromatic transition bonds. The appearance of a broad shoulder near 250 nm in the carboxylated graphene sample indicated the success of the chosen functionalization strategy. An additional characteristic peak at 280 nm in the antibody-conjugated graphene sample was attributed to the successful grafting of antibodies on graphene sheets.

The FE-SEM results of the bare (SPE) and antibody conjugated (Ab-fG-SPE) electrodes are shown in Fig. 3. These studies revealed

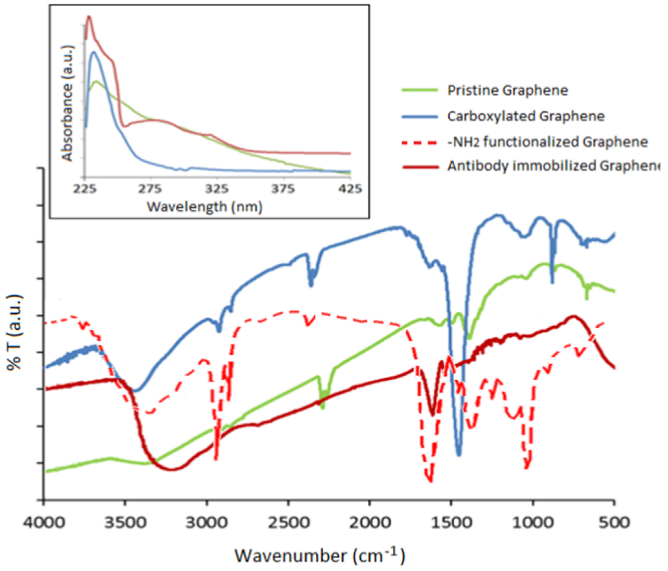

Fig. 2. FTIR and UV–vis spectra (inset image) of pristine graphene, carboxylated graphene, and antibody-immobilized graphene.

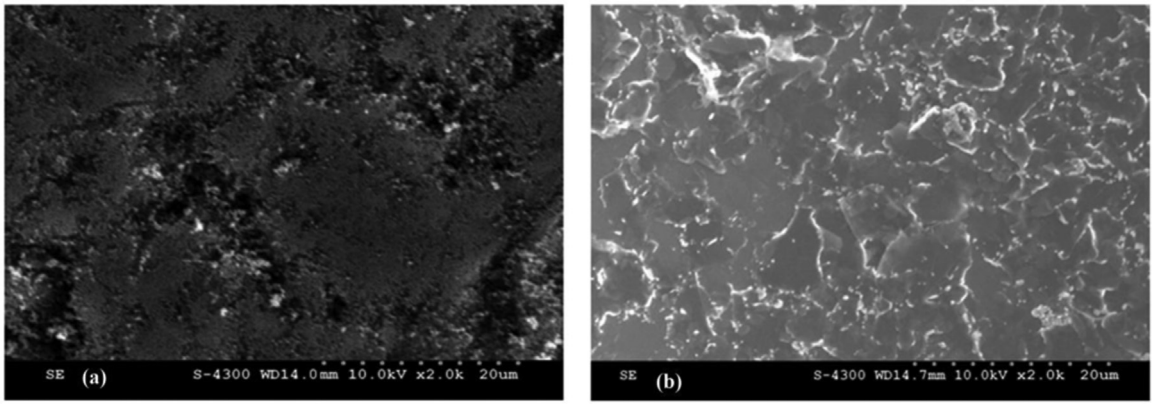

Fig. 3. (a) FE-SEM analysis of bare SPE (SPE) and (b) FE-SEM analysis of antibody-conjugated fG-SPE (Ab-fG-SPE).(For interpretation of the references to color in this figure, the reader is referred to the web version of this article.)

the information about modifications at the electrode surface. The bioelectrode 'Ab-fG-SPE' was characterized with a fairly homogenous surface elucidating the deposition of globular proteinaceous antibodies. The different steps of biosensor formation were also characterized with the AFM investigations (Supplementary Information, Fig. S1). The bare SPE was characterized with a relatively rough line profile ($\pm$ 200 nm) (Fig. S1a), whereas its evident modification (Fig. S1b) with the functionalized graphene smoothened the surface to a significant extent ($\pm$ 60 nm). The AFM of the native antibody particles displayed them as nanosized (4–5 nm) globules (Fig. S1c). The immobilization of the antibodies on the fG-SPE could be firmly assessed from Fig. S1d and S1e in which the modification of the graphene electrode is visualized with the protein particles. The roughness of this final biosensor surface was also limited to $\pm$ 40 nm. Investigations by confocal laser scanning microscopic (CLSM) also helped verify a successful formation of the Ab-fG-SPE electrodes. The fluorescence imaging of a dye (FITC) attached antibody sample and an Ab-fG-SPE electrode are shown in Fig. S2. These samples were excited with a laser light of 488 nm. The dye tagged antibody molecules exhibited their characteristic emission profile (Fig. S2a). An intact fluorescence from the bioconjugated graphene electrode highlighted a successful assembly of the antibodies (Fig. S2b). Note that we did not observe any fluorescence signal for the bare SPE, C-SPE, and fG-SPE. Therefore, the observed emission from the proposed biosensor electrode should be clearly indicative of a successful attachment of the antibody.

3.2. Cyclic voltammetry studies

Cyclic voltammetry (CV) studies of the electrodes were conducted during the different steps of the biosensor development (Fig. 4a). A parallelogram shape of the graphene (carboxylated G-SPE) electrode depicted the internal resistance of the electrode. The capacitance can be attributed to the charge and discharge of the double layer. The presence of various functional groups in the material could be accounted for by the pseudocapacitance effect in the cyclic voltammograms (e.g., Karthika et al., 2012). The carboxylated graphene surface displayed a more prominent pseudocapacitance effect due to the presence of more oxidizing oxygen functionalities (Karthika et al., 2012). The same effect was also observed in the 2-ABA functionalized graphene but to a relatively lesser extent. The functionalization of G-SPE with $-NH_2$ groups (from 2-ABA) resulted in improved peak characteristics in terms of positive peak potential due to the enhancement in the catalytic activity (Navaee and Salimi, 2015). Further, attachment of the antibodies caused a decrease in the peak intensities as the protein molecules hindered the charge transfer due to their insulating nature (Han et al., 2011; Choudhary et al., 2013). The pseudocapacitance effect was also abated due to the decreased presence of the electrochemically active species (i.e. -COOH), a reduced tunneling of the charge, and passivation of the background current (Chen et al., 2011). The CV studies highlighted successful modification of SPE with the antibodies. The effect of antibody-antigen binding was also reflected in CV patterns, where an anodic shift was observed due to the presence of electron-withdrawing

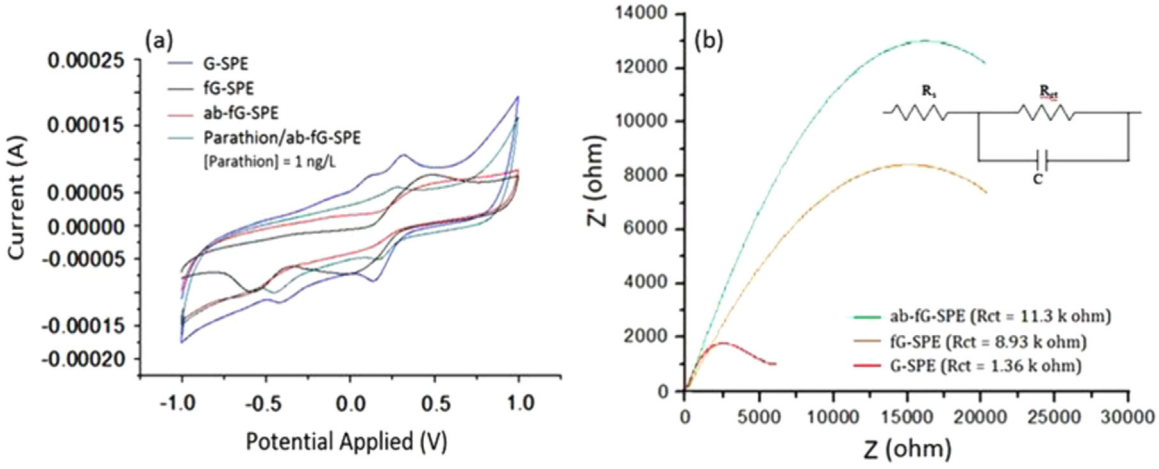

Fig. 4. (a) Cyclic voltammograms of graphene modified SPE (G-SPE), 2-ABA-functionalized G-SPE (fG-SPE), antibody-conjugated fG-SPE (Ab-fG-SPE), and antigen-antibody-fG-SPE (parathion/Ab-fG-SPE) and (b) Nyquist plots of graphene-modified SPE (G-SPE), 2-ABA-functionalized G-SPE (fG-SPE), and antibody-immobilized fG-SPE (Ab-fG-SPE).

parathion molecules (Cutler et al., 2002).

The effective surface area of electrodes at different modification steps was calculated using the method described by Yola et al. (2014a) (Eq. (1)).

$$i_p = 2.69 \times 10^5 A\, n^{3/2} D^{1/2} C\, v^{1/2} \quad (1)$$

where i_p- peak current, A- electrode surface area, n- number of electrons transferred, D- diffusion coefficient, C- concentration of redox media, and v- scan rate. The estimated surface areas for the G-SPE, fG-SPE, and Ab-fG-SPE electrodes were 0.047, 0.031, and 0.032 cm^2, respectively.

3.3. Impedimetric detection of parathion

Electrochemical impedance data are commonly expressed by the Nyquist plots in which the imaginary impedance component (Z", out-of-phase) is compared against the real impedance component (Z', in-phase) at different excitation frequencies. The parameter 'charge transfer resistance' or the R_{ct} denotes the real component of impedance. Based on the nature of the measuring signal, the impedance immunosensors can be classified into 'Capacitive' and 'Faradaic' categories. The former works in the absence of the redox probe to measure capacitive current under a small amplitude sinusoidal voltage signal. The latter suits where the surface of the electrode is partially or wholly covered by a non-insulating layer such as the antibody molecules. These electrodes are thus able to catalyze a redox probe to measure the R_{ct} parameter. Antibody-antigen (Ab-Ag) interactions tend to increase the value of R_{ct} as the Faradaic reaction becomes increasingly hindered. In general, the Faradaic impedimetric immunosensors can exhibit enhanced sensitivity to the Ab-Ag interactions.

Electrochemical impedance spectroscopy (EIS) studies were conducted to evaluate the kinetics of charge transport by graphene modified SPE (G-SPE), 2-ABA functionalized G-SPE (fG-SPE), and the antibody-immobilized fG-SPE (Ab-fG-SPE). The resultant data in the form of Nyquist plots are shown in Fig. 4b. These studies were carried out in the frequency range of 1 KHz–1 MHz. The real impedance component (Z') was plotted against the imaginary impedance component (Z"). The values of R_{ct} were computed by fitting and modelling the impedance data in a Randles equivalent circuit. As indicated in Fig. 4b, the semicircle diameter for the carboxylated graphene increased after its immobilization with the anti-parathion antibodies. The antibody molecules immobilized at the surface of electrode acted as a dielectric layer which hindered the diffusion of the redox probe, accounting for the observed increase in the R_{ct} value.

The Ab-fG-SPE was used for the impedimetric analysis of parathion in a dynamic concentration range of 0.01–10^4 ng/L. Nyquist plots generated during the EIS analysis of varying parathion concentrations are shown in Fig. 5a. The semicircular diameter showed a gradual increase with the increasing antigen (parathion) concentration. The antibody-antigen binding at the electrode surface altered the properties of the dielectric layer to restrict the charge transport across the redox probe and electrode surface. Consequently, as the Faradic process was hindered, the values of R_{ct} increased linearly in proportional to the parathion concentration over a range (0.1–10^3 ng/L) (Fig. 5b). Note that the R_{ct} values below that range (< 0.1 ng/L) were not distinguishable from the baseline values, while those above that range ($> 10^3$ ng/L) remained almost constant due to the signal saturation. Here, the explanations for an observed increase in the R_{ct} value of the biosensor electrode upon its exposure to the analyte solution can be sought for by considering the electronegative nature of the parathion molecules. Parathion is negatively charged due to the presence of p-nitrophenol (as an organic radical). The presence of the electron withdrawing groups can facilitate trapping of more and more electrons within the antigen layer itself. It thus destructs the 2D and 3D electron conducting pathways to transport less charges to the graphene electrode through antigen-antibody layer.

The limit of detection (LOD) was computed by the formula: LOD = K × s.d. / S. The value of K was taken as 3, s.d was computed as the standard deviation of the blank sample, and S was the slope of the calibration curve. The LOD of the developed Ab-fG-SPE immunosensor was estimated to be 0.052 ng/L, which is better than those of the previously reported electrochemical methods (Table 1). The specificity of the proposed technique was investigated by analyzing 10 ng/L parathion in the presence of elevated ratio concentrations [1 (parathion): 100 (paraoxon, malathion, and monochrotophos)] of other organophosphate pesticides. The results of this analysis are shown in Fig. S3. The tested electrodes did not respond to the above non-specific pesticides, suggesting the desired specificity of the used antibody.

3.4. Reproducibility, regeneration and stability of the sensor

For testing the reproducibility of the developed biosensor electrodes, a number of the Ab-fG-SPE electrodes (five) were used to analyze a fixed concentration (10 ng/L) of parathion. Fig. S4 shows the response of these electrodes. No significant change (1–1.5%) was found in sensor response, suggesting excellent reproducibility of the proposed electrodes. The regeneration efficiency of the biosensor surface was investigated by washing a used sensing electrode with 10 mM of Glycine-HCl solution (pH 2.5) (Andersson et al., 1999). The regenerated sensor was tested again for the detection of parathion. The output characteristics (R_{ct}) of the regenerated sensor were found fairly consistent (signal attenuation of less than 10%) upto the five recycling steps. We also investigated the long-term stability of the developed sensor

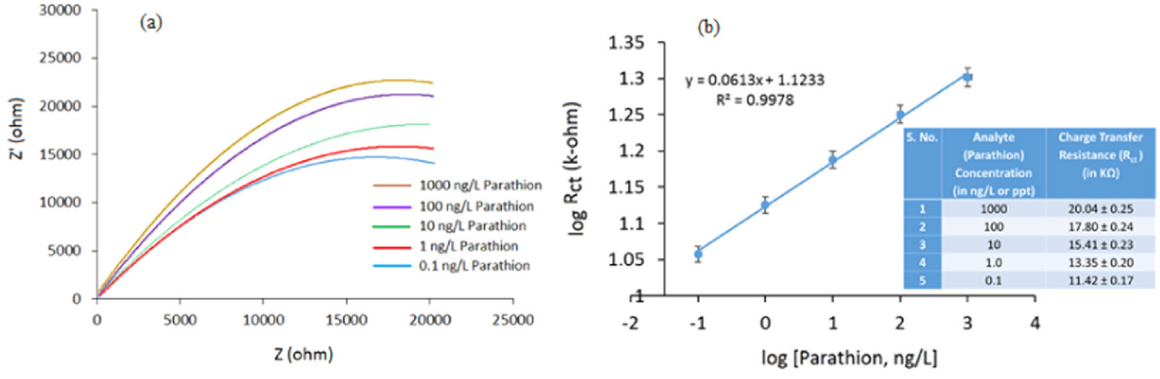

Fig. 5. (a) Nyquist plots observed during the EIS analysis of varying concentrations of parathion and (b) Log-log calibration plot depicting R_{ct} values as a function of parathion concentration along with tabular data to show estimated R_{ct} values for different analyte concentrations.

Table 1
Performance comparison of different immunosensing systems for parathion (and other pesticides) between this study and previous reports.

Sensing Material	Transduction method	Limit of detection	Detection range	Sensor stability	Reference
Gold nanoparticles/ multiwalled carbon nanotube (MWCNT) film	Amperometry (monitoring of peak current in cyclic voltammograms)	1 ng/mL for methyl parathion	5.0–200 ng/mL	30 days	Du et al. (2010)
Graphite nanoplatelet (xGnPs)–chitosan cross-linked composite	Voltammetry	0.158 nM for chloropyrifos	0.1 nM–0.1 μM	10 days	Ion et al. (2010)
Electrochemically reduced graphene oxide and Nafion hybrid nanocomposite	Electrochemical impedance spectroscopy (EIS)	2.0 ng/mL for dichlorvos	5.0–100 ng/mL	30 days	Wu et al. (2013)
Carbon nanotube-Web (CNT-Web)-modified glassy carbon (GC) electrode	Differential pulse voltammetry (DPV)	1 nM for methyl parathion	20–1000 nM	30 days	Musameh et al. (2013)
Molecularly imprinted polymer–ionic liquid–graphene composite film-coated glassy carbon electrode	DPV	6 nM for methyl parathion	0.010–7.0 μM	30 days	Zhao et al. (2013)
Graphene-Nafion/GCE	Electrochemical stripping voltammetry (ESV)	1.6 ng/mL for methyl parathion	0.02–20 μg/mL	NA	Xue et al. (2013)
Graphene nanosheets (GNs)/gadolinium Prussian Blue analogue modified glassy carbon electrode	ESV	1 nM for methyl parathion	0.008–10 μM	30 days	Li et al. (2014)
Nano Metal-organic framework (NMOF)/ Indium-tin oxide (ITO)	EIS	0.1 ng/mL for parathion	0.1–20 ng/mL	25 days	Deep et al. (2015)
Graphene oxide (GO)–chitosan (CS) composite film	Cyclic voltammetry (CV)	1.2 nM for carbaryl/tri-chlorfon	10–100 nM	15 days	Zhou et al. (2015)
Reduced graphene oxide-Au nanoparticles-β-cyclodextrin/Prussian blue chitosan nanocomposites	CV	1.15 pg/mL for carbaryl	4.3–1000 pg/mL	28 days	Zhao et al., (2015)
Ag/Cu Graphene nano-composite	Differential pulse adsorptive stripping voltammetric	4.0 pM for chlorpyrifos	0.01–100 nM	30 days	Sreedhar et al. (2015)
Graphene-Co_3O_4 composite	DPV	11 nM	0.4–20 μM	30 days	Liu et al. (2015)
Anti-parathion antibody immobilized onto graphene sheet-modified, screen-printed electrodes	EIS	0.052 ng/L	0.1–1000 ng/L	50 days	This Work

electrodes. For this, a number of electrodes were stored at refrigerated conditions (4 °C) and used periodically for the analysis of parathion at an interval of 10 days. As shown in Fig. S5, an excellent stability of the Ab-fG-SPE electrodes was realized. The sensor response was fairly stable (reduction in the sensor's output signal smaller than 5%) even after 50 days of storage.

3.5. Quantification of parathion in spiked real samples

In order to evaluate the developed sensor's performance in practical applications, the method was extended for the quantification of parathion in food samples (tomato and carrot). The sample preparation was carried out by treating 5 g of the properly cleaned and homogenized tomato/carrot samples with 20 mL of diethyl ether. The mixtures were stirred for 1 h, and the supernatants were filtered through a 0.22 μm hydrophilic membrane. The collected extracts were evaporated to dryness and then resuspended in 5 mL of ethanol. The standard addition method was employed to estimate the recovery of parathion in the real (food) samples. The concentrations of parathion were hence determined from the extracted food samples (after spiking with its standards) by the Ab-fG-SPE impedimetric sensor. The results were also validated via HPLC, for which the conditions were as follows: column: Li-Chrosorb RP-18 (Merck); pre-column: RP-18 (Merck); mobile phase: 70/30 (v/v) acetonitrile/water; injectionvolume: 20 μL; and detection wavelength: 270 nm. Table 1S shows the parathion analysis data in tomato and carrot samples using the Ab-fG-SPE sensor and HPLC. We obtained excellent mean percentage recoveries (%R) with satisfactory relative standard deviations. The obtained data thus confirmed a high precision of the proposed procedure. Furthermore, the analysis results were also in good agreement with the HLPC data.

4. Conclusions

In summary, a new graphene based impedimetric biosensor has been developed for highly sensitive and specific quantification of parathion. Using a convenient processing route, graphene was drop-cast onto screen-printed electrodes (SPE), which were then electro-functionalized with 2-ABA. These modified SPE with available $–NH_2$ functional groups were conjugated with anti-parathion antibodies to realize the desired sensor design. The use of graphene as a support material provided a large surface area for antibody immobilization. Further, the adopted strategy of conjugating the F_c region of the antibodies with the sensor surface ensured the availability of the F_{ab} region for effective antigen targeting, i.e., parathion molecules. The analytical performance of the proposed sensor was then assessed through reliable and feasible evaluations in terms of both sensitivity (low limit of detection) and specificity (against other pesticides). The practicality of the sensor was further verified through the analysis of real (food) samples spiked with parathion and cross-validation against standard (HPLC) method.

Acknowledgements

JM acknowledges the University Grant Commission, India for her research fellowship. The work was funded through CSIR India grant OMEGA/PSC0202/2.2.5. The authors are also thankful to the Director of CSIR-CSIO Chandigarh for infrastructure facilities. KHK acknowledges partial support by a National Research Foundation of Korea (NRF) grant funded by the Ministry of Education, Science and Technology (MEST) (No. 2009–0093848).

Appendix A. Supplementary material

Supplementary data associated with this article can be found in the online version at http://dx.doi.org/10.1016/j.bios.2016.04.058.

References

Akyıldırım, O., Medetalibeyoğlu, H., Manap, S., Beytur, M., Tokalı, F.S., Yola, M.L., Atar, N., 2015. Electrochemical sensor based on graphene oxide/iron nanoparticles for the analysis of quercetin. Int. J. Electrochem. Sci. 10, 7743–7753.

Andersson, K., Areskoug, D., Hardenborg, E., 1999. Exploring buffer space for molecular interactions. J. Mol. Recognit. 12 (5), 310–315.

Apetrei, I., Popa, C., Apetrei, C., Tutunaru, D., 2014. Biosensors based on graphene modified screen-printed electrodes for the detection of catecholamines. Rom. Biotech. Lett. 19 (5), 9802.

Aragay, G., Pino, F., Merkoçi, A., 2012. Nanomaterials for sensing and destroying pesticides. Chem. Rev. 112 (10), 5317–5338.

Arora, P., Sindhu, A., Dilbaghi, N., Chaudhury, A., 2011. Biosensors as innovative tools for the detection of food borne pathogens. Biosens. Bioelectron. 28 (1), 1–12.

Aslan, S., Cakir, Z., Emet, M., Serinken, M., Karcioglu, O., Kandis, H., Uzkeser, M., 2011. Acute abdomen associated with organophosphate poisoning. J. Emerg. Med. 41 (5), 507–512.

Atar, N., Yola, M.L., Eren, T., 2016. Sensitive determination of citrinin based on molecular imprinted electrochemical sensor. Appl. Surf. Sci. 362, 315–322.

Atar, N., Eren, T., Yola, M.L., Karimi-Maleh, H., Demirdögena, B., 2015. Magnetic iron oxide and iron oxide@gold nanoparticle anchored nitrogen and sulfur-functionalized reduced graphene oxide electrocatalyst for methanol oxidation. RSC Adv. 5, 26402–26409.

Audrey, S., Beatriz, P.-S., Jean-Louis, M., 2012. Biosensors for pesticide detection: new trends. Am. J. Anal. Chem. 3 (3), 210–232.

Bhardwaj, S.K., Bhardwaj, N., Mohanta, G.C., Kumar, P., Sharma, A.L., Kim, K.-H., Deep, A., 2015. Immunosensing of atrazine with antibody-functionalized Cu-MOF conducting thin films. ACS Appl. Mater. Inter 7 (47), 26124–26130.

Bontidean, I., Ahlqvist, J., Mulchandani, A., Chen, W., Bae, W., Mehra, R.K., Mortari, A., Csöregi, E., 2003. Novel synthetic phytochelatin-based capacitive biosensor for heavy metal ion detection. Biosens. Bioelectron. 18 (5), 547–553.

Bourigua, S., Hnaien, M., Bessueille, F., Lagarde, F., Dzyadevych, S., Maaref, A., Bausells, J., Errachid, A., Renault, N.J., 2010. Impedimetric immunosensor based on SWCNT-COOH modified gold microelectrodes for label-free detection of deep venous thrombosis biomarker. Biosens. Bioelectron. 26 (4), 1278–1282.

Chauhan, N., Narang, J., Jain, U., 2016. Amperometric acetylcholinesterase biosensor for pesticides monitoring utilising iron oxide nanoparticles and poly (indole-5-carboxylic acid). J. Exp. Nanosci. 1 (2), 111–122.

Chen, Y., Zhang, X., Zhang, D., Yua, P., Ma, Y., 2011. High performance supercapacitors based on reduced graphene oxide in aqueous and ionic liquid electrolytes. Carbon 49 (2) 573–380.

Cherian, S., Gupta, R.K., Mullin, B.C., Thundat, T., 2003. Detection of heavy metal ions using protein-functionalized microcantilever sensors. Biosens. Bioelectron. 19 (5), 411–416.

Chhabra, V.A., Deep, A., Kaur, R., Kumar, R., 2012. Functionalization of graphene using carboxylation process. Int. J. Sci. Emerg. Technol. 4, 13–19.

Choudhary, M., Kumar, V., Singh, A., Singh, M.P., Kaur, S., Reddy, G.B., Pasricha, R., Singh, S.P., Arora, K., 2013. Graphene oxide based label free ultrasensitive immunosensor for lung cancer biomarker, hTERT. J. Biosens. Bioelectron. 4, 143.

Cutler, C.A., Burrell, A.K., Officer, D.L., Too, C.O., Wallace, G.G., 2002. Effect of electron withdrawing or donating substituents on the photovoltaic performance of polythiophenes. Synt. Met. 128 (1), 35–42.

Deep, A., Bhardwaj, S.K., Paul, A., Kim, K.-H., Kumar, P., 2015. Surface assembly of nano-metal organic framework on amine functionalized indium tin oxide substrate for impedimetric sensing of parathion. Biosens. Bioelectron. 65, 226–231.

Du, D., Wang, J., Smith, J.N., Timchalk, C., Lin, Y., 2009. Biomonitoring of organophosphorus agent exposure by reactivation of cholinesterase enzyme based on carbon nanotube-enhanced flow-injection amperometric detection. Anal. Chem. 81 (22), 9314–9320.

Du, D., Ye, X., Cai, J., Liu, J., Zhang, A., 2010. Acetylcholinesterase biosensor design based on carbon nanotube-encapsulated polypyrrole and polyaniline copolymer for amperometric detection of organophosphates. Biosens. Bioelectron. 25 (11), 2503–2508.

Dzyadevych, S.V., Soldatkin, A.P., Korpan, Y.I., Arkhypova, V.N., Anna, V., Chovelon, J.-M., Martelet, C., Jaffrezic-Renault, N., 2003. Biosensors based on enzyme field-effect transistors for determination of some substrates and inhibitors. Anal. Bioanal. Chem. 377 (3), 496–506.

Goicolea, M.A., Gómez-Caballero, A., Barrio, R.J., 2011. New materials in electrochemical sensors for pesticides monitoring. Pestic. Strateg. Pestic. Anal., 333–358. http://dx.doi.org/10.5772/565.

Gong, J., Miao, X., Wan, H., Song, D., 2012. Facile synthesis of zirconia nanoparticles-decorated graphene hybrid nanosheets for an enzymeless methyl parathion sensor. Sens. Actuators B. Chem. 162 (1), 341–347.

Gong, J., Miao, X., Zhou, T., Zhang, L., 2011. An enzymeless organophosphate pesticide sensor using Au nanoparticle-decorated graphene hybrid nanosheet as solid-phase extraction. Talanta 85 (3), 1344–1349.

Han, J., Zhuo, Y., Chai, Y.Q., Mao, L., Yuan, Y.L., Yuan, R., 2011. Highly conducting gold nanoparticles-graphene nanohybrid films for ultrasensitive detection of carcinoembryonic antigen. Talanta 85 (1), 130–135.

Ion, A.C., Ion, I., Culetu, A., Gherase, D., Moldovan, C.A., Iosub, R., Dinescu, A., 2010. Acetylcholinesterase voltammetric biosensors based on carbon nanostructure-chitosan composite material for organophosphate pesticides. Mater. Sci. Eng. C 30 (6), 817–821.

Jeon, I.-Y., Shin, Y.-R., Sohn, G.-J., Choi, H.-J., Bae, S.-Y., Mahmood, J., Jung, S.-M., Seo, J.-M., Kim, M.-J., Chang, D.W., 2012. Edge-carboxylated graphene nanosheets via ball milling. Proc. Natl. Acad. Sci. 109 (15), 5588–5593.

Karthika, P., Rajalakshmi, N., Dhathathreyan, K.S., 2012. Functionalized exfoliated graphene oxide as supercapacitor electrodes. Soft Nanosci. Lett. 2 (4), 59–66.

Khosraviani, M., Pavlov, A.R., Flowers, G.C., Blake, D.A., 1998. Detection of heavy metals by immunoassay: optimization and validation of a rapid, portable assay for ionic cadmium. Environ. Sci. Technol. 32 (1), 137–142.

Kotan, G., Kardaş, F., Yokuş, O.A., Akyıldırım, O., Saral, H., Eren, T., Yola, M.L., Atar, N., 2016. A novel determination of curcumin via Ru@Au nanoparticle decorated nitrogen and sulfur-functionalized reduced graphene oxide nanomaterials. Anal. Methods 8, 401–408.

Kumar, P., Deep, A., Kim, K.-H., 2015. Metal organic frameworks for sensing applications. Tr. Anal. Chem. 73, 39–53.

Kumar, P., Kumar, P., Deep, A., Bharadwaj, L.M., 2012. Doped zinc-organic framework for sensing of pesticide. Adv. Mater. Res. 488, 1543–1546.

Li, P., Lei, N., Sheadel, D.A., Xu, J., Xue, W., 2012. Integration of nanosensors into a sealed microchannel in a hybrid lab-on-a-chip device. Sens. Actuators B Chem. 166, 870–877.

Li, Y., Xu, M., Li, P., Dong, J., Ai, S., 2014. Nonenzymatic sensing of methyl parathion based on graphene/gadolinium Prussian Blue analogue nanocomposite modified glassy carbon electrode. Anal. Methods 6 (7), 2157–2162.

Liu, G., Lin, Y., 2005. Electrochemical sensor for organophosphate pesticides and nerve agents using zirconia nanoparticles as selective sorbents. Anal. Chem. 77 (18), 5894–5901.

Liu, T., Su, H., Qu, X., Ju, P., Cui, L., Ai, S., 2011a. Acetylcholinesterase biosensor based on 3-carboxyphenylboronic acid/reduced graphene oxide–gold nanocomposites modified electrode for amperometric detection of organophosphorus and carbamate pesticides. Sens. Actuators B. Chem. 160 (1), 1255–1261.

Liu, T., Xu, M., Yin, H., Ai, S., Qu, X., Zong, S., 2011b. A glassy carbon electrode modified with graphene and tyrosinase immobilized on platinum nanoparticles for sensing organophosphorus pesticides. Microchim. Acta 175 (1–2), 129–135.

Liu, F.M., Du, Y.Q., Cheng, Y.M., Yin, W., Hou, C.J., Huo, D.Q., Chen, C., Fa, H.B., 2015. A selective and sensitive sensor based on highly dispersed cobalt porphyrin-Co_3O_4-graphene oxide nanocomposites for the detection of methyl parathion. J. Solid State Electr. 20 (3), 599–607.

Mattiasson, B., 1997. Cell-based biosensors for environmental monitoring with special reference to heavy metal analysis. Res. Microbiol. 148 (6), 533.

Mulchandani, A., Chen, W., Mulchandani, P., Wang, J., Rogers, K.R., 2001. Biosensors for direct determination of organophosphate pesticides. Biosens. Bioelectron. 16 (4), 225–230.

Musameh, M., Notivoli, M.R., Hickey, M., Huynh, C.P., Hawkins, S.C., Yousef, J.M., Kyratzis, I.L., 2013. Carbon nanotube-Web modified electrodes for ultrasensitive detection of organophosphate pesticides. Electrochim. Acta 101, 209–215.

Navaee, A., Salimi, A., 2015. Efficient amine functionalization of graphene oxide through the Bucherer reaction: an extraordinary metal-free electrocatalyst for the oxygen reduction reaction. RSC Adv. 5 (74), 59874–59880.

Ping, J., Wang, Y., Fan, K., Wu, J., Ying, Y., 2011. Direct electrochemical reduction of graphene oxide on ionic liquid doped screen-printed electrode and its electrochemical biosensing application. Biosens. Bioelectron. 28 (1), 204–209.

Preininger, C., Wolfbeis, O.S., 1996. Disposable cuvette test with integrated sensor layer for enzymatic determination of heavy metals. Biosens. Bioelectron. 11 (10), 981–990.

Rosi, N.L., Mirkin, C.A., 2005. Nanostructures in biodiagnostics. Chem. Rev. 105 (4), 1547–1562.

Shao, Y., Wang, J., Wu, H., Liu, J., Aksay, I.A., Lin, Y., 2010. Graphene based electrochemical sensors and biosensors: a review. Electroanalysis 22 (10), 1027–1036.

Sreedhar, N., Kumar, M.S., Krishnaveni, K., 2015. Sensitive determination of chlorpyrifos using Ag/Cu alloy nanoparticles and graphene composite paste electrode. Sens. Actuators B Chem. 210, 475–482.

Singh, A., Flounders, A., Volponi, J., Ashley, C., Wally, K., Schoeniger, J., 1999. Development of sensors for direct detection of organophosphates. Part I: immobilization, characterization and stabilization of acetylcholinesterase and organophosphate hydrolase on silica supports. Biosens. Bioelectron. 14 (8), 703–713.

Song, W., Li, H., Liu, H., Wu, Z., Qiang, W., Xu, D., 2013. Fabrication of streptavidin functionalized silver nanoparticle decorated graphene and its application in disposable electrochemical sensor for immunoglobulin E. Electrochem. Commun. 31, 16–19.

Sukirtha, T., Usharani, M., 2013. Production and qualitative analysis of biosurfactant and biodegradation of the organophosphate by Nocardia mediterranie. J. Bioremed. Biodegrad. 4 (6), 198–205.

Suri, C.R., Boro, R., Nangia, Y., Gandhi, S., Sharma, P., Wangoo, N., Rajesh, K., Shekhawat, G., 2009. Immunoanalytical techniques for analyzing pesticides in the environment. Tr. Anal. Chem. 28 (1), 29–39.

Takahashi, Y., Shevchuk, A.I., Novak, P., Murakami, Y., Shiku, H., Korchev, Y.E., Matsue, T., 2010. Simultaneous noncontact topography and electrochemical imaging by SECM/SICM featuring ion current feedback regulation. J. Am. Chem.

Soc. 132 (29), 10118–10126.
Tuteja, S.K., Kukkar, M., Suri, C., Paul, A., Deep, A., 2015. One step in-situ synthesis of amine functionalized graphene for immunosensing of cardiac marker cTnI. Biosens. Bioelectron. 66, 129–135.
Wang, S., Sun, H., Ang, H.-M., Tadé, M., 2013. Adsorptive remediation of environmental pollutants using novel graphene-based nanomaterials. J. Chem. Eng. 226, 336–347.
Wang, Y., Shao, Y., Matson, D.W., Li, J., Lin, Y., 2010. Nitrogen-doped graphene and its application in electrochemical biosensing. ACS Nano 4 (4), 1790–1798.
Wen, L.-L., Wang, F., Leng, X.-K., Wang, C.-G., Wang, L.-Y., Gong, J.-M., Li, D.-F., 2010. Efficient detection of organophosphate pesticide based on a metal- organic framework derived from biphenyltetracarboxylic acid. Cryst. Growth Des. 10 (7), 2835–2838.
Wu, S., Huang, F., Lan, X., Wang, X., Wang, J., Meng, C., 2013. Electrochemically reduced graphene oxide and Nafion nanocomposite for ultralow potential detection of organophosphate pesticide. Sens. Actuators B Chem. 177, 724–729.
Xue, R., Kang, T.-F., Lu, L.-P., Cheng, S.-Y., 2013. Electrochemical sensor based on the graphene-nafion matrix for sensitive determination of organophosphorus pesticides. Anal. Lett. 46 (1), 131–141.
Yang, J., Yu, J.-H., Strickler, J.R., Chang, W.-J., Gunasekaran, S., 2013. Nickel nanoparticle–chitosan-reduced graphene oxide-modified screen-printed electrodes for enzyme-free glucose sensing in portable microfluidic devices. Biosens. Bioelectron. 47, 530–538.
Yola, M.L., Eren, T., Atar, N., 2014a. A novel and sensitive electrochemical DNA biosensor based on Fe@ Au nanoparticles decorated graphene oxide. Electrochim. Acta 125, 38–47.
Yola, M.L., Gupta, V.K., Atar, N., 2016. New molecular imprinted voltammetric sensor for determination of ochratoxin A. Mat. Sci. Eng. C 61, 368–375.
Yola, M.L., Gupta, V.K., Eren, T., Şen, A.E., Atar, N., 2014b. A novel electro analytical nanosensor based on graphene oxide/silver nanoparticles for simultaneous determination of quercetin and morin. Electrochim. Acta 120, 204–211.
Yola, M.L., Atar, N., Eren, T., Karimi-Maleh, H., Wang, S., 2015. Sensitive and selective determination of aqueous triclosan based on gold nanoparticles on polyoxometalate/reduced graphene oxide nanohybrid. RSC Adv. 5, 65953–65962.
Zhao, L., Zhao, F., Zeng, B., 2013. Electrochemical determination of methyl parathion using a molecularly imprinted polymer–ionic liquid–graphene composite film coated electrode. Sens. Actuators B Chem. 176, 818–824.
Zhao, H., Ji, X., Wang, B., Wang, N., Li, X., Ni, R., Ren, J., 2015. An ultra-sensitive acetylcholinesterase biosensor based on reduced graphene oxide-Au nanoparticles-β-cyclodextrin/Prussian blue-chitosan nanocomposites for organophosphorus pesticides detection. Biosens. Bioelectron. 65, 23–30.
Zhou, N., Li, C., Mo, R., Zhang, P., He, L., Nie, F., Su, W., Liu, S., Gao, J., Shao, H., 2015. A graphene/enzyme-based electrochemical sensor for sensitive detection of organophosphorus pesticides. Surf. Rev. Lett. 23 (2), 1550103.

Web reference

⟨http://consumerresources.in/2015/04/16/the-pesticides-who-classifies-as-cancer-causing-are-used-widely-in-india/⟩. Last accessed on 8/4/2016.